frontiers in Chemistry

ORIGINAL RESEARCH
published: 15 March 2022
doi: 10.3389/fchem.2022.840133

Mussel-Inspired Magnetic Dissolving Pulp Fibers Toward the Adsorption and Degradation of Organic Dyes

Jiawei Yang[1,2], *Shengchang Lu*[1,3], *Hui Wu*[1,2], *Huichao Hu*[1,2], *Qingxian Miao*[1,2], *Liulian Huang*[1,2], *Lihui Chen*[1,2]* *and Yonghao Ni*[1,4]

[1]College of Material Engineering, Fujian Agriculture and Forestry University, Fuzhou, China, [2]National Forestry and Grassland Administration Key Laboratory of Plant Fiber Functional Materials, Fuzhou, China, [3]School of Forestry, Henan Agricultural University, Zhengzhou, China, [4]Department of Chemical Engineering, Limerick Pulp and Paper Centre, University of New Brunswick, Fredericton, NB, Canada

In this work, a simple synthetic method was used to prepare a new type of magnetic dissolving pulp (MDP) @polydopamine (PDA) fibers. The hydroxyl groups of the fibers were converted into carboxyl groups after succinylation. Fe_3O_4 nanoparticles were grown *in situ* on the fibers. The prepared MDP@PDA fibers have catalytic reduction efficiency and adsorption performance for methylene blue organic dyes, and it has been thoroughly tested under various pH conditions. Fe_3O_4@PDA fibers have high reusability, are easy to separate, and regenerate quickly. The catalytic and adsorption efficiency barely decreases after repeated use. The surface of dissolving pulp fibers with a functionalized multifunctional PDA coating is used to create multifunctional catalysts and adsorbent materials. This study presents a very useful and convenient method for the synthesis and adjustment of MDP@PDA fibers, which have a wide range of potential applications in catalysis and wastewater treatment.

Keywords: magnetic dissolving, absorbance, degradation, organic dye, synthetic method

OPEN ACCESS

Edited by:
Aiqin Wang,
Lanzhou Institute of Chemical Physics, (CAS), China

Reviewed by:
Bin Yan,
Sichuan University, China
Xin Jia,
Shihezi University, China

***Correspondence:**
Lihui Chen
lihuichen66@126.com

Specialty section:
This article was submitted to Green and Sustainable Chemistry, a section of the journal Frontiers in Chemistry

Received: *20 December 2021*
Accepted: *24 January 2022*
Published: *15 March 2022*

Citation:
Yang J, Lu S, Wu H, Hu H, Miao Q, Huang L, Chen L and Ni Y (2022) Mussel-Inspired Magnetic Dissolving Pulp Fibers Toward the Adsorption and Degradation of Organic Dyes. Front. Chem. 10:840133. doi: 10.3389/fchem.2022.840133

INTRODUCTION

Water pollution by organic contaminants has become a serious environmental issue and received significant attention (Wang et al., 2009; Xie et al., 2014). Among many organic pollutants, it is critical to address pollution issues with organic dyes. Water contamination by dyes from various industries, such as textiles, leather, and dyestuffs, has gotten more attention because the dyes in these industrial wastewaters are toxic, carcinogenic, and nonbiodegradable (Yuanyuan Liu et al., 2015; Cho et al., 2015). As a result, a variety of technologies, including adsorption (Hossain et al., 2021), photocatalytic degradation, chemical reduction or chemical oxidation, membrane filtration, flocculation, and electro-oxidation, have been used to remove these contaminants (Panizza and Cerisola, 2009; Ali, 2012). Adsorption is one of the most effective methods to treat organic dyes, and it is widely used because of its relatively low cost and easy operation. Various adsorbents have been designed to remove dyes in water and have considerable adsorption capacities, such as activated carbon (Tang et al., 2017; Zhang et al., 2019; Soares et al., 2021), functional carbon materials (Magno et al., 2020; Xing et al., 2020; Zhang et al., 2020), composite hydrogel (Srivastava and Roy Choudhury, 2021), and metal oxide (Rastogi et al., 2017; Xu et al., 2020; Şerban and Enesca, 2020). Among these methods, chemistry reduction has gained popularity because of its ease of use, high efficiency, clean processing, and low cost. The chemical reduction of various dyes with $NaBH_4$ is an important, safe, and environmentally friendly alternative. This process is thermodynamically advantageous in the

absence of a catalyst, but kinetics is difficult. Because the redox potential difference between the electron donor and acceptor hinders electron transfer, the electron transfer step is dynamic. As a result, an efficient catalyst with a moderate oxidation–reduction potential can serve as an electron shuttle, facilitating electron transfer.

Redox mediators (RMs) play a key role in improving the performance of electron-receiving priority pollutants. As RMs can be reversibly oxidized and reduced (Coletti et al., 2012; Lentini et al., 2014), they can be used as electron transfer means in multiple redox reactions, increasing the reaction rate by one or more orders of magnitude. Because water-soluble RMs that are washed away with wastewater are typically used, RMs must be added continuously, raising the processing cost. Furthermore, the RMs in the effluent will cause secondary pollution. As a result, the ideal RM for catalytic pigment degradation should promote sewage purification while minimizing secondary pollution. RM immobilized on a suitable carrier shows great potential as a catalyst in these processes (Du et al., 2017).

Inspired by the marine mussels, which have the unique wet adhesion capability, polydopamine (PDA) has attracted strong interest as a biomimetic polymer (Tang et al., 2021) and a universal surface modification agent for various materials with a broad range of applications (Zeng et al., 2010; Bandara et al., 2012; Wang et al., 2018; Lin et al., 2019; Lin et al., 2020; Wang et al., 2020; Xiang et al., 2020; Lu et al., 2021). PDA-functionalized hybrid materials were recently developed as a novel nanostructured adsorbent for dye removal. In the field of wastewater treatment, Chen et al. developed a PDA modified cyclodextrin polymer adsorbent (Chen et al., 2020). Mu et al. described a chitosan/PDA@C@magnetic fly ash adsorbent bead for Ag (I) ion adsorption in aqueous solutions (Mu et al., 2020). With the help of PDA catechol groups, these adsorbents demonstrated excellent cationic dye and metal ion adsorption (Xie et al., 2014). Dissolving pulp (DP) is a high-grade cellulose pulp (90%–98% cellulose content), with low hemicellulose, lignin, and resin content (Peng et al., 2012; Arce et al., 2020), which has been steadily increasing in popularity over the last decade (Llano et al., 2018; Liu et al., 2021). Cellulose is regarded as the most abundant and renewable natural resource on the earth and promising as adsorbents owing to the inherent porous structure. The functionalization of cellulose tends to lead to an even higher adsorption capacity for days (Kim et al., 2017; Li et al., 2018; Lu et al., 2018).

Herein, we present a facile synthetic method of *in situ* reductions to prepare MDP@PDA fibers, where PDA acts as a coating to adsorb the dyes (Lee et al., 2007). It is celebrated that under mild solution conditions, dopamine can automatically self-polymerize into PDA, which can be used as a binder and coating on various substrates, as inspired by the unique underwater adhesion properties of marine mussel foot proteins (Lee et al., 2007; Zeng et al., 2010; Bandara et al., 2012). MDP@PDA fibers are easy to separate in water because of its magnetism. Thus, a simple method for synthesizing novel MDP@PDA fibers with obviously fast adsorption ability for methylene blue (MB) at different pH values and easily separated from the water was

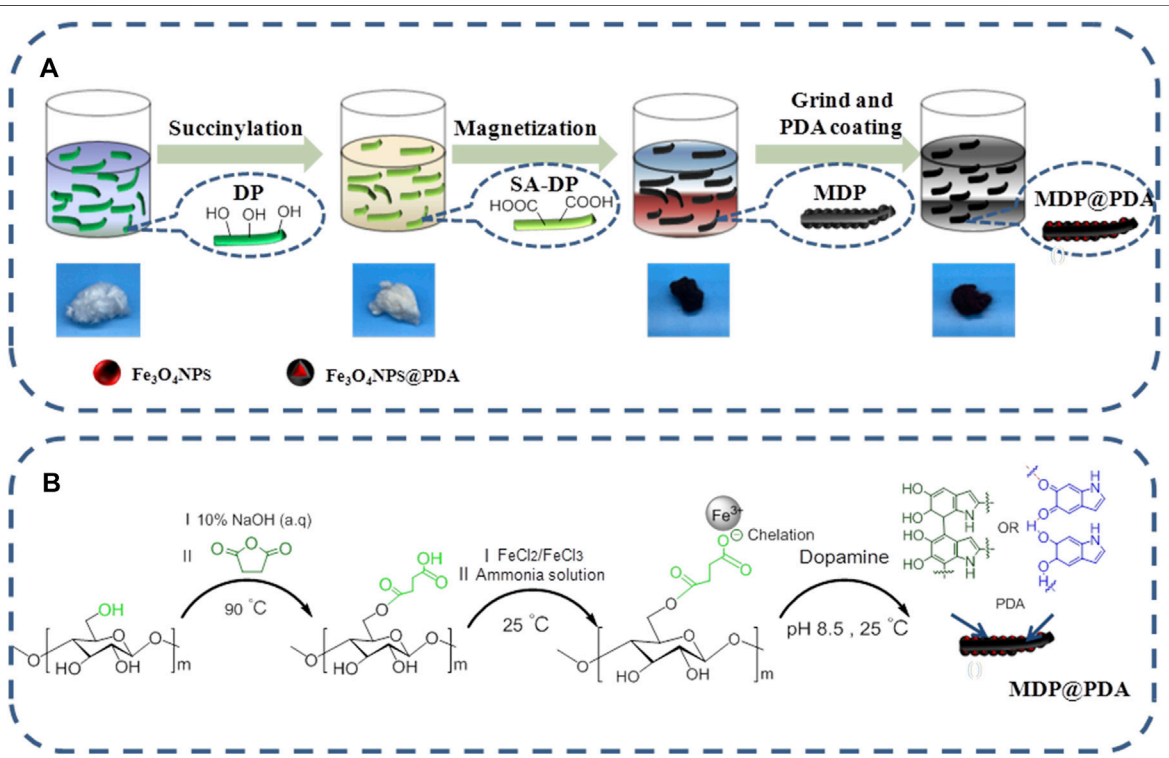

FIGURE 1 | (A) Scheme of synthesis of MDP@PDA fibers. **(B)** The synthesis of MDP@PDA.

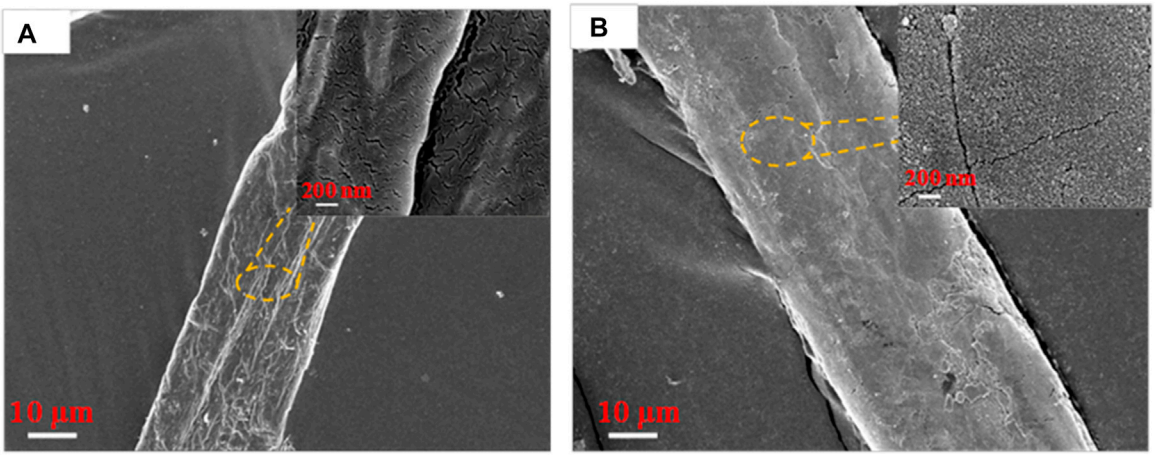

FIGURE 2 | SEM images of fiber surface: **(A)** DP and **(B)** MDP@PDA fibers.

developed in this work. The modified fibers have exceptional cyclic performance.

MATERIALS AND METHODS

Materials

DP was procured from Fujian Qinshang Paper Industry Co., Ltd. Succinic anhydride, iron (II) chloride ($FeCl_2$), and ammonia solution (25–30% NH_3) were obtained from Innochem. Aladdin provided dopamine hydrochloride, MB, pyridine, iron (III) chloride ($FeCl_3$) hexahydrate, and sodium chloride (NaCl). Macklin and Xilong Scientific supplied sodium hydroxide and toluene, respectively. Ultrapure water was obtained using LabTower EDI 15 system (Thermo, USA) and was applied for all experiments.

Succinylation of DP

The DP board was dispersed into a cotton shape with fiber dissociator, and a total of 0.5 g of the DPs was immersed in an aqueous solution of 10 wt% NaOH (50 mL) for 24 h. Then, the samples were repeatedly washed with absolute ethanol until a solution with neutral pH was obtained. After removing the moisture from the pulps in a vacuum drying oven (40°C), the DPs were used for further reaction. Pretreated DP (0.5 g, 9.1 mmol of active-OH groups (Roy et al., 2005)) was reacted with succinic anhydride (2.5 g, 25 mmol) at 90°C for 24 h in 10 mL of a mixed solvent containing toluene (35 mL) and pyridine. Then, the pulp samples were removed from the reaction and washed with toluene at least three times and soon afterward with acetone about five times before using a vacuum drying oven (40°C). Finally, the succinylation (SA)–DP was allowed to store in a desiccator until further analysis or functionalization.

Preparation of Magnetic DP@PDA Fibers

The magnetic dissolving pulps (MDPs) were fabricated through the *in situ* synthesis of Fe_3O_4, located in the porous of carboxylated DPs (Xu et al., 2012). By stirring under nitrogen,

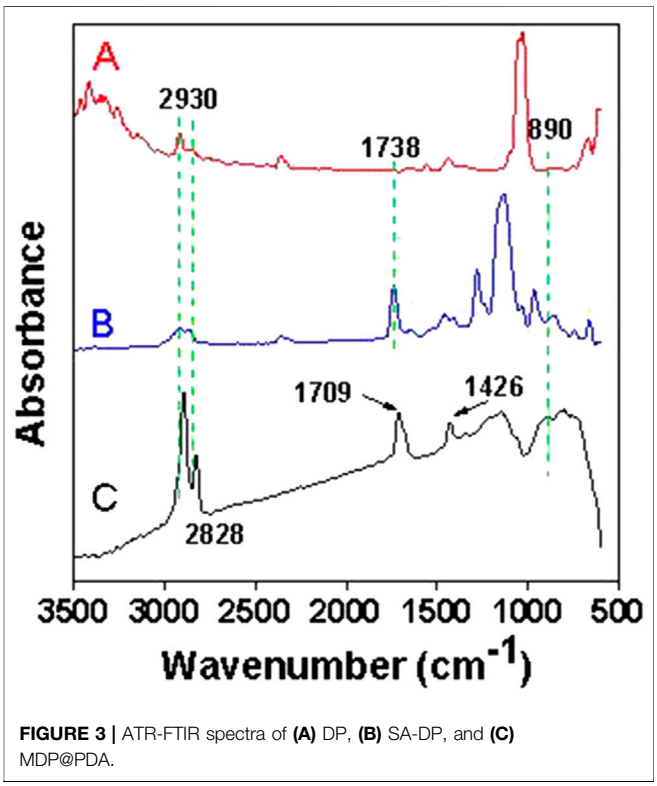

FIGURE 3 | ATR-FTIR spectra of **(A)** DP, **(B)** SA-DP, and **(C)** MDP@PDA.

the succinylated DPs (0.5 g) were added in a mixture solution of $FeCl_2$ (2.7 g, 0.1 mol) and $FeCl_3$ (0.63 g, 0.05 mol) (mole ratio $FeCl_3$:$FeCl_2$ = 2:1, and ultrapure water was 50 mL) in a 200 mL two-necked flask. Then, while stirring, an excessive ammonia solution (approximately 50 mL) was added and reacted for 1 h. The obtained reaction product was filtered and washed with a large amount of deionized water to remove any remaining ammonia and impurities before being freeze-dried. Afterward, a dopamine hydrochloride (0.25 mmol) solution dissolved in

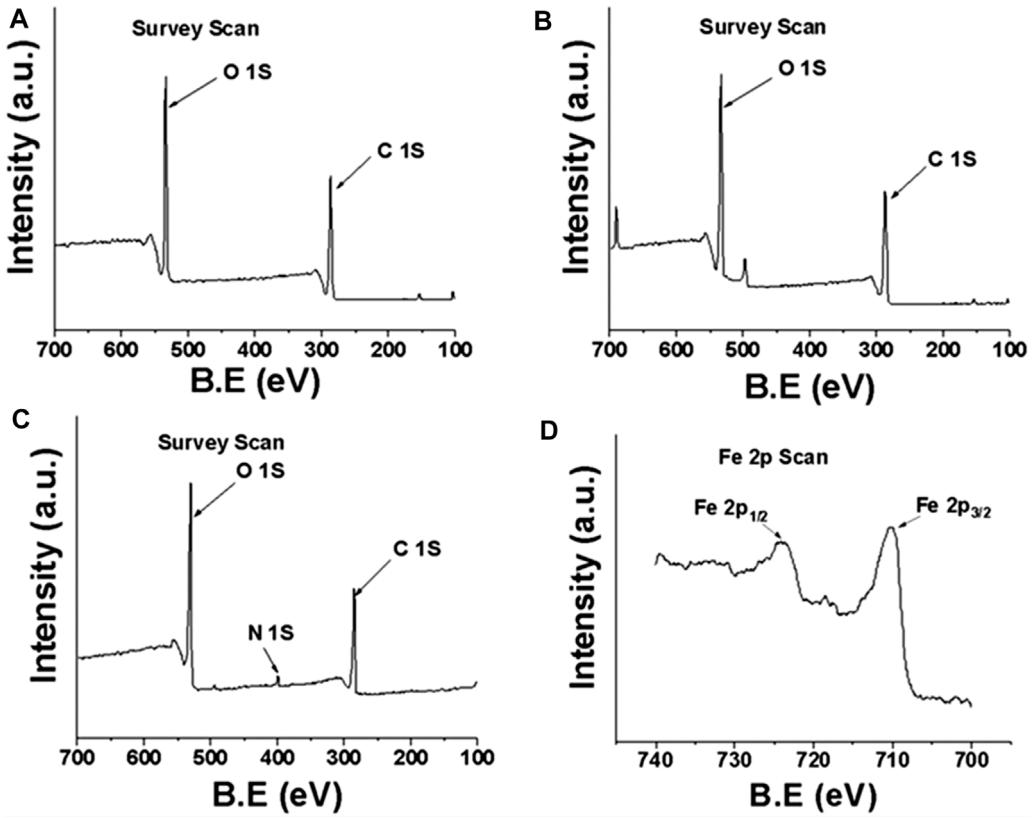

FIGURE 4 | XPS survey scan: **(A)** DP, **(B)** SA-DP, **(C)** MDP@PDA, and **(D)** Fe 2p XPS spectra of MDP@PDA.

phosphate-buffered saline (pH 8.5, titrated with NaOH) was prepared (Park et al., 2020). Subsequently, the prepared MDP fibers (0.5 g) were mixed into the dopamine solution in a 200-mL single-neck flask and reacted on an on-air table for 8 h.

Characterizations

Fourier transform infrared spectroscopy (FTIR) spectra of the dried DP, SA-DP, MDP@PDA, and MB adsorbed MDP@PDA were recorded on a Bruker VERTEX 70 FTIR spectrometer in the region of 400–4,000 cm^{-1}. The surface morphologies of the synthesized MDP@PDA samples were achieved using a field emission scanning electron microscopy at a voltage of 5 kV. On a Kratos Axis Ultra spectrometer set to 30 eV, the X-ray photoelectron spectroscopy (XPS) spectra were recorded using Al Kα radiation. A vibrating sample magnetometer was used to measure the magnetic properties (VSM, 7,307; Lakeshore, USA). The DP and MDP@PDA fibers were subjected to thermogravimetric analysis using the synchronous thermal analyzer (Mettler TGA/DSC3+, Switzerland). Five milligrams of sample was placed in the crucible and heated from 30°C to 600°C at a rate of $10°C \cdot min^{-1}$ under N_2 flow. The experiment of Zeta potential was performed using a similar method as previous literature (Zhang et al., 2018); briefly, 0.1 $g \cdot L^{-1}$ DP and MDP@PDA fibers dispersion was analyzed by Malvern Zetasizer (NanoZS90X, United Kingdom).

Adsorption Experiments

A 20 mg portion of MDP@PDA fibers was added into 10 mL MB aqueous solution (pH 6.2, 40 $mg \cdot L^{-1}$) under constant stirring at room temperature. To monitor the adsorption process, the effect of pH (3, 5, 7, 9) was investigated with 20 mg MDP@PDA and dye initial concentration of 40 $mg \cdot L^{-1}$, respectively; NaCl (0.05, 0.1, and 0.2 $g \cdot L^{-1}$) was used to evaluate the influences of electrolyte on dye removal efficiency; the UV-vis absorption spectra of MB at various pH and ion concentrations were recorded. The adsorbents were separated from the solution with an external magnet at the end of adsorption. Before the next desorption–adsorption cycle; the recycled adsorbents were washed with fresh $NaBH_4$ aqueous solution (2 mL, 1.5 $mmol \cdot L^{-1}$) and then washed with ethanol and ultrapure water at least three times. The formula for calculating the decolorization ratio (D_{color} R, %) is as follows:

$$D_{color}\ R = \frac{C_0 - C_1}{C_0} \times 100\% \quad (1)$$

where C_0 and C_1 are the dye concentrations ($mg \cdot L^{-1}$) in the initial reaction and postreaction solution, respectively.

Catalytic Reduction Experiments

A 10-mg portion of MDP@PDA fibers was added to a 10 mL MB aqueous solution. Subsequently, 0.1 mL of fresh $NaBH_4$ aqueous solution (0.1 $mol \cdot L^{-1}$) was injected into the solution under stirring. The blue color of MB gradually vanished by catalytic

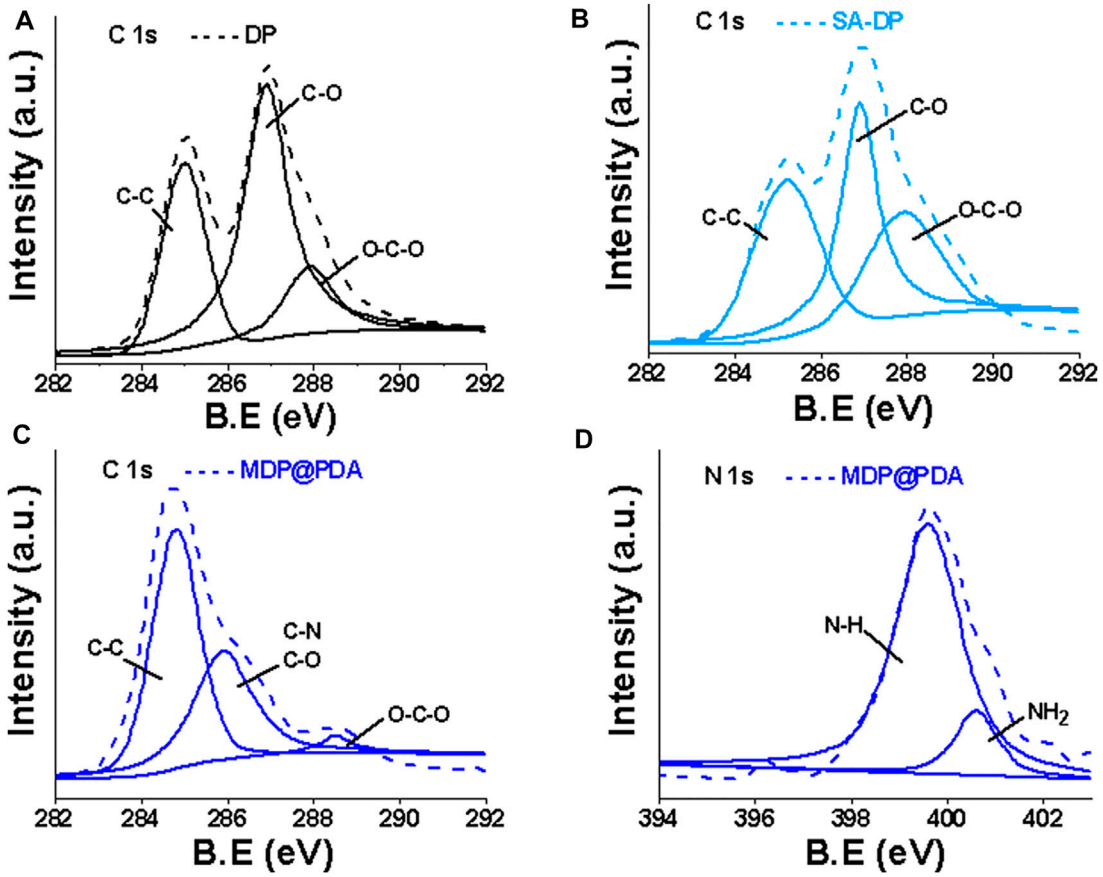

FIGURE 5 | The C 1s XPS spectra of **(A,B)** DP and SA-DP, the C 1 s, and N 1s XPS spectra of **(C,D)** MDP@PDA.

reduction, and the decolorization ratio was calculated by measuring the changes in the absorbance at 665 nm with a UV-vis spectrophotometer based on **Equation 1**.

RESULTS AND DISCUSSION

Synthesis and Characterizations of Materials

Our mussel-inspired strategy, as described in **Figure 1**, requests the adjunct of the dopamine molecules onto the DP fibers, which is composed of β-glucose units containing primary alcohol (-OH) groups, and we exploited these alcohol groups for functionalizing the finer surface by succinylation. The alcohol (-OH) groups of the glucose unit, on the other hand, are not readily available for functionalization because the majority of them form intermolecular hydrogen bonds with the attachment of alcohol (-OH) groups, leaving only a few available for surface reaction (Lee et al., 2015). After being succinylated, the DP fibers were treated with a 10% NaOH aqueous solution to disrupt the extensive hydrogen bonds between fibers by deprotonating the primary alcohol (-OH) groups of glucose units, and we can conclude that the alkali treatment of DP fibers was able to increase the degree of succinylation (Tankhiwale and Bajpai, 2008; Islam et al., 2018). Typically, SA-DP fibers were first synthesized through a succinic anhydride and used pyridine as anhydride catalyst in toluene solution, and the white fibers turned yellowish. Afterward, the SA-DP was added to the iron ion (the ratio of Fe^{3+} and Fe^{2+} is 2: 1) mixed solution, and then the iron ions were reduced *in situ* by adding ammonia to make the fibers black and magnetic. Finally, the MDP fibers were blended into dopamine solution and adjusted the pH to 8.5 to make the dopamine self-aggregate on the fiber surface (**Figure 1A**); fibers still appeared black.

The microscopic morphology of DP and MDP@PDA was characterized by SEM to observe the fiber surface after the reaction. The results showed that, when compared with DP in **Figure 2A**, nanosized PDA particles are generated on the surface of MDP@PDA in **Figure 2B**, and a large amount of them agglomerates (Peng et al., 2012). Because of dopamine's catechol and amino-functional structure, which can form covalent and noncovalent bond interactions with organic–inorganic surfaces, the PDA cross-linked layer is attached to the surface of fibers (Lee et al., 2006; Lee et al., 2007). To confirm the chemical structural changes of the DP after experiencing their successive reaction, infrared absorbance experiments were performed on DP, SA-DP, and MDP@PDA, The result of ATR-FTIR spectra is shown in **Figure 3**. In all ATR-FTIR spectra, the peaks 2,930 and 2,828 cm^{-1} are related to methylene asymmetry and symmetric stretching vibration (Otsuka

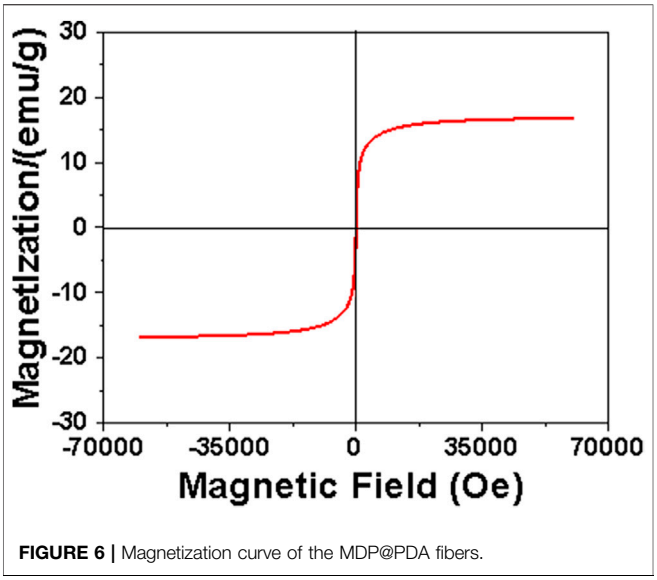

FIGURE 6 | Magnetization curve of the MDP@PDA fibers.

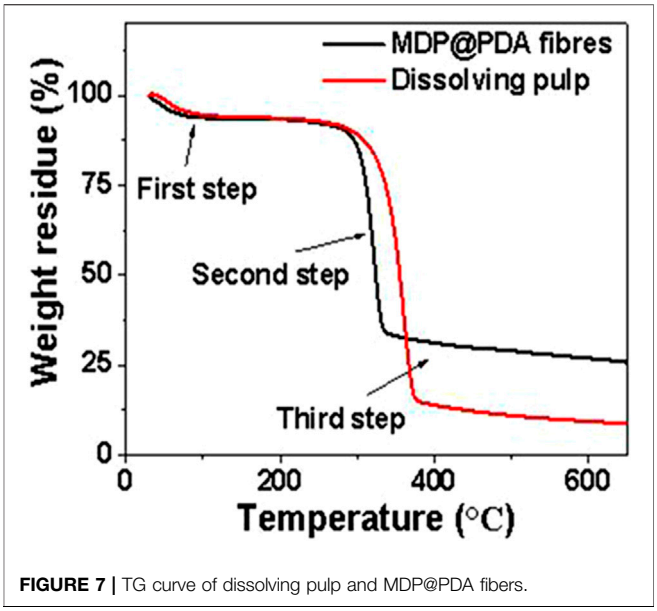

FIGURE 7 | TG curve of dissolving pulp and MDP@PDA fibers.

et al., 2017), which explained the existence of cellulose backbone structure. In **Figure 3B**, compared with DP in **Figure 3A**, the absorbance observed at 1,738 cm^{-1} revealed the formation of carbonyl structures, especially the C=O (Ding et al., 2017). What's more, the result showed in **Supplementary Figure S2** indicated that MB was adsorbed onto the MDP@PDA fibres successfully.

XPS was used to characterize the surface elemental composition and chemical bonding information of the fibers. The XPS survey of DP fibers and SA-DP fibers showed the peak for C 1s (~286 eV) and O 1s (~531 eV) only. MDP@PDA fiber surface was reflected by the appearance of the N 1s (~400 eV), Fe $2p_{1/2}$ (~724.1 eV), and Fe $2p_{3/2}$ (~710 eV) (Liu et al., 2016) in **Figure 4**. Further characterization by XPS was performed to probe the surface functionalization of the fibers as shown in **Figure 5**. The high-resolution C1s spectra of DP, SA-DP, and MDP@PDA fibers are shown in **Figures 5A–C**, components that were assigned to C-C (285.1 eV), C-O (286.9 eV), and O-C-O (288.4 eV). The high-resolution N 1s spectra of MDP@PDA fibers are shown in **Figure 5D**.

We observed changes in the ratio of chemical bonds C-C, C-O (mainly from cellulose structure), and O-C-O (mainly from SA modification). The N 1s region can fit three peaks at 401.3, 399.8, and 398.6 eV. The first 401.3 eV can be assigned to the amine group (R-NH_2), which could be due to the presence of a small amount of physically self-assembled dopamine alongside polymeric dopamine. Simultaneously, the peaks at 399.8 and 398.6 eV can be attributed to PDA's substituted amine (R-NH-R, or indolyl) and imino group (=N-R). The XPS results demonstrated the successful deposition of the PDA coating and the formation of magnetized DP fibers.

Figure 6 presents the magnetization curve of the MDP@PDA fibers, the saturation magnetization value was 16.7 emu/g, indicating that the MDP@PDA fibers have good magnetic properties and were higher than the DP fibers (Lin et al., 2016).

To determine the thermal stability of cellulose and PDA, thermal analysis was performed on fiber and PDA, respectively. The thermal analysis curves of DP and MDP@PDA fibers with three steps are displayed in **Figure 7**. Specifically, the first step was primarily water evaporation, with a decomposition temperature of 30°C–126°C and a mass loss of approximately 6.4%. In the second step, the significant mass loss from 200°C to 400°C resulted from the rupture of cellulose polymeric chain. Obviously, the weight losses of DP and MDP@PDA fibers were approximately 86% and 61%, respectively. The third step of mass loss was assigned to the oxidative pyrolysis decomposition, the MDP mass loss reached 74% from 340°C to 600°C, and the DP mass loss reached 91% from 400°C to 600°C (Zhang et al., 2021). Compared with DP fibers, the MDP@PDA fibers retained relatively good thermal stability after chemical and magnetic modification; furthermore, it can be known from the thermal analysis curve that the content of magnetic nanoparticles on the fibers was approximately 17%.

Adsorption Performance

The adsorption of MB molecules by MDP@PDA fibers is a prerequisite for the catalytic reduction of MB in the $NaBH_4$ system. Adsorption tests were also carried out to gain a better understanding of the catalytic reduction of MB by MDP@PDA fibers prepared as a catalytic reduction mediator and $NaBH_4$ as a catalyst. **Figure 8A** depicts the time-dependent UV-vis spectra of the prepared MDP@PDA fiber used as an adsorbent for MB solution adsorption. The MB absorption peak began to decrease at 15 min and disappeared at 60 min, indicating that the MB in the solution was primarily absorbed by MDP@PDA fibers. Obviously, MB is the common cationic dyes (Ge et al., 2012), in order to evaluate the surface charge properly of the DP fibers and MDP@PDA fibers for the capability of MB adsorption; the zeta potential of DP fibers and MDP@PDA fibers were -6.6 ± 0.5 and -20.6 ± 2.3 mV at the pH value of 6.2, demonstrating that modified fibers exhibited more pronounced electrostatic effect on MB compared with pristine fibers as shown in **Supplementary Figure S1**. NaCl was used to investigate the

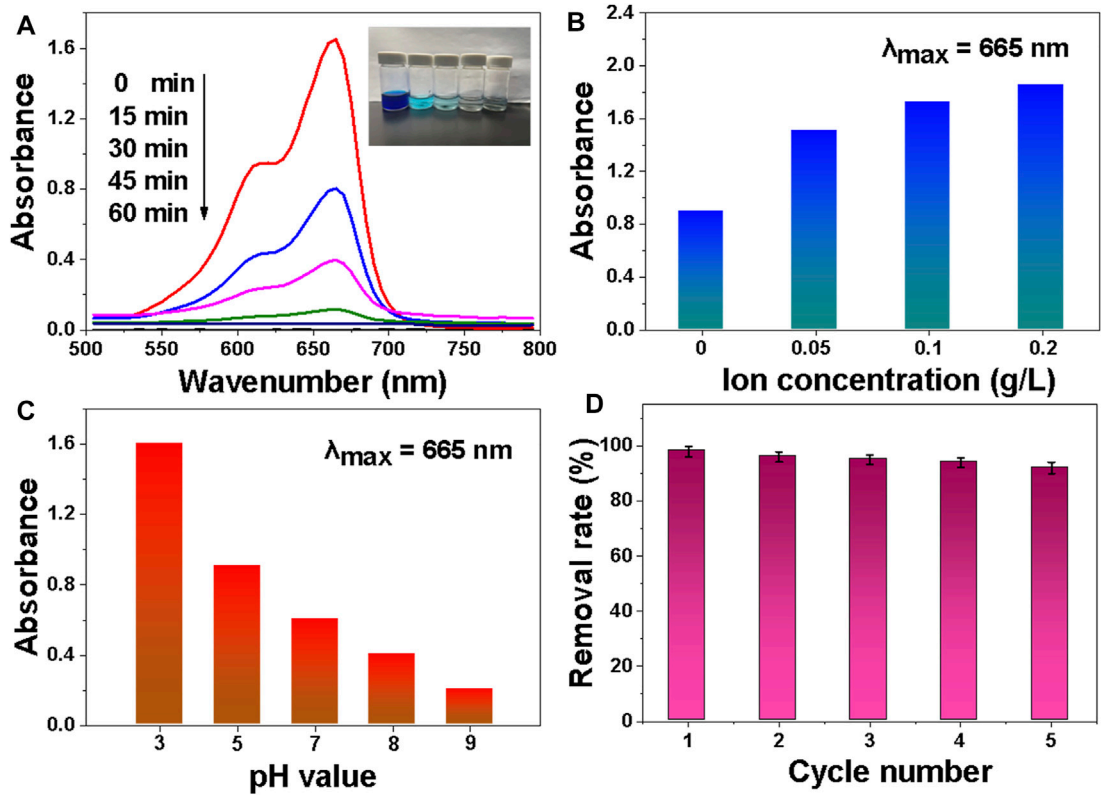

FIGURE 8 | (A) Successive UV-vis absorption spectra of MB aqueous solution (40 mg · L^{-1}) in the presence of MDP@PDA fibers. **(B)** Influence of ion concentration on MB adsorption performance. **(C)** The influence of pH value on MB adsorption performance. **(D)** The removal rate of MB with MDP@PDA fibers in different cycle numbers.

TABLE 1 | Comparison of the comprehensive properties of absorbents for MB adsorption.

Adsorbents	MB adsorption capacity ($mg \cdot g^{-1}$)	Magnetic	Catalytic reduction	Reference
Fe_3O_4@PDA-Ag	~ 4	Yes	Yes	Cui et al. (2018)
PDA microspheres	90.7	No	No	Fu et al. (2015)
CNC–ALG	256.41	No	No	Mohammed et al. (2015)
LPMCC/LPH-0.6	51.54	No	No	Dai et al. (2021)
Cellulose/TiO_2	0.8	No	No	Jo et al. (2017)
MDP@PDA	~ 20	Yes	Yes	This work

effect of ionic strength on the adsorption performance of MB solution. As the result shown in **Figure 8B**, with the increase in NaCl ion concentration, the adsorption performance of the MDP@PDA fibers gradually decreased. As the previous reports (Mahmoodi et al., 2011; Metin et al., 2013; Lin Liu et al., 2015), the competitive effect of MB solution with salt ions (Na^+ and Cl^-) could be used to explain such results, and the competitive was evident as the NaCl concentration increase, leading to a decrease in the adsorption capacity of MDP@PDA fibers for MB. Meanwhile, this result indicated that the adsorption might be caused by electrostatic interaction between MDP@PDA fibers and dye molecules. **Figure 8C** shows that the pH value of the solution has a great influence on the adsorption of MB by MDP@PDA fibers. The better the adsorption effect, the higher the pH value. Because of the synergistic effects of electrostatic interaction, interaction and hydrogen bonding between PDA layers and organic dyes could be a possible adsorption mechanism. There is more electrostatic interaction when the pH value is high. The adsorbents' recyclability was also assessed. **Figure 8D** shows that the MDP@PDA fibers could be recycled and reused for at least five times with a stable adsorption of more than 90%. Adsorption capacity is one of the critical indicators for evaluating adsorbents (Hokkanen et al., 2016). **Table 1** shows the comparison of the comprehensive properties of absorbents for MB adsorption. Some adsorbents display better adsorption capacity (30–300 $mg \cdot g^{-1}$) (Fu et al., 2015; Mohammed et al., 2015; Dai et al., 2021) for MB than that of the MDP@PDA fibers (20 $mg \cdot g^{-1}$). However, most of the other adsorbents have limitations in magnetic properties and catalytic reduction performance by comparing with MDP@PDA fibers. Thus, these features may endow MDP@PDA fibers to have

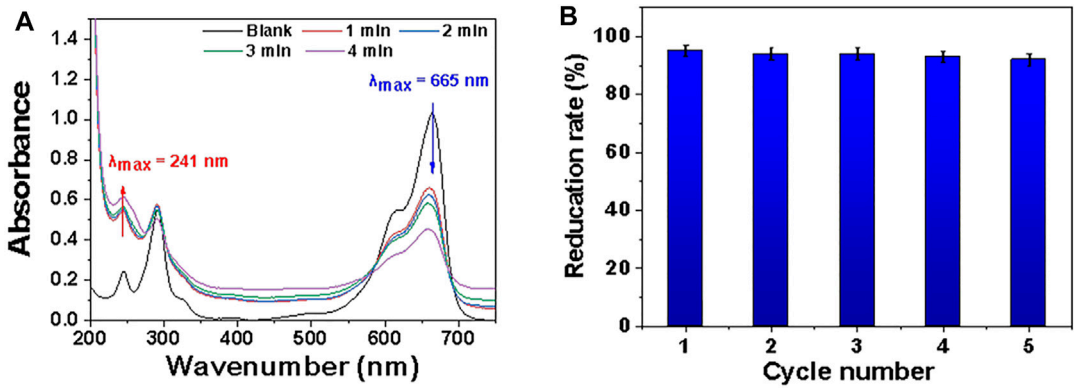

FIGURE 9 | (A) Successive UV-vis absorption spectra UV of MB catalytic reduction process under different time conditions. The blank sample is measured after 40 mg · L^{-1} MB solution diluted 10 times. **(B)** Reduction rate of MB with MDP@PDA fibers in different cycle number.

potential applications with an easy-to-operate approach in wastewater treatment fields.

Catalytic Reduction Performance

Figure 9 shows that in the MB/$NaBH_4$ system with MDP@PDA fibers as a catalyst, MB faded to completely colorless in 4 min, and while the absorbance of MB at 665 nm gradually decreased, a new absorption peak appeared at 246 nm, indicating the reduction product LMB. The addition of MDP@PDA significantly increased the rate of degradation of MB solution.

The prepared MDP@PDA fibers showed high reduction activity for MB solution (pH 3.0), although their adsorption activity for MB removal was still relatively low. The catalytic reduction of MB molecules by $NaBH_4$ in the presence of Fe_3O_4 nanoparticles has been considered as an electrochemical mechanism, in which Fe_3O_4 nanoparticles act as electronic relays for MB and BH_4^-. Only on the surface of Fe_3O_4 nanoparticles can the catalytic reaction occur, where electrons are transferred from BH_4^- to MB molecules. As a result, the catalytic reduction reaction requires the adsorption of MB molecules by the catalyst. The electrostatic interaction between the PDA layer and the MB molecule, as well as the π–π stacking interaction, dominate the adsorption mechanism of the prepared MDP@PDA fiber. After adding $NaBH_4$ solution, BH_4^- ions will gradually adsorb to the surface of MDP@PDA fibers through competitive adsorption. BH_4^- ions are nucleophilic, have high electron injection capabilities, and can cathodically polarize Fe_3O_4 nanoparticles on the catalyst surface.

CONCLUSION

In this work, MDP@PDA fibers have been prepared through a simple and easy strategy. Fe_3O_4 nanoparticles are grown *in situ* on the surface of the DP fibers and then self-polymerized on the fiber surface by DOPA to prepare MDP@PDA fiber. The MDP@PDA fiber showed enhanced catalytic activity based on $NaBH_4$ reduction of MB as a model reaction. The chemical composition of the MDP@PDA fiber, in which the stable and immobilized Fe_3O_4 nanoparticles and the PDA layer have a synergistic effect, can be attributed to the excellent catalytic performance. MDP@PDA fiber has excellent recyclability because of its inherent magnetism, and it is catalytic, and adsorption efficiency does not decrease significantly after repeated use. Mussels inspired the functionalization of the PDA coating on the MDP fiber to develop multifunctional catalyst and adsorbent materials. Our research results provide a very useful and convenient method for the synthesis and adjustment of MDP@PDA fibers, which can significantly improve their catalytic and adsorption properties for organic dyes, and have huge potential applications in catalysis and wastewater treatment.

DATA AVAILABILITY STATEMENT

The original contributions presented in the study are included in the article/**Supplementary Material**, further inquiries can be directed to the corresponding author.

AUTHOR CONTRIBUTIONS

JY planned and executed the main experiments, analyzed the data, and wrote the main manuscript. SL performed some experiments and revised the manuscript. HW, HH, QM, LH, LC and YN analysed the results and revised the manuscript. All authors critically reviewed and approved the final manuscript.

ACKNOWLEDGMENTS

We would like to thank the financial support from National key research and development plan (Grant Nos. 2019YFC1905903), National Natural Science Foundation of China (31971612, 31700520).

SUPPLEMENTARY MATERIAL

The Supplementary Material for this article can be found online at: https://www.frontiersin.org/articles/10.3389/fchem.2022.840133/full#supplementary-material

REFERENCES

Ali, I. (2012). New Generation Adsorbents for Water Treatment. *Chem. Rev.* 112, 5073–5091. doi:10.1021/cr300133d

Arce, C., Llano, T., García, P., and Coz, A. (2020). Technical and Environmental Improvement of the Bleaching Sequence of Dissolving Pulp for Fibre Production. *Cellulose* 27, 4079–4090. doi:10.1007/s10570-020-03065-1

Bandara, N., Zeng, H., and Wu, J. (2012). Marine Mussel Adhesion: Biochemistry, Mechanisms, and Biomimetics. *J. Adhes. Sci. Technol.* 27, 2139–2162. doi:10.1080/01694243.2012.697703

Chen, H., Zhou, Y., Wang, J., Lu, J., and Zhou, Y. (2020). Polydopamine Modified Cyclodextrin Polymer as Efficient Adsorbent for Removing Cationic Dyes and Cu2+. *J. Hazard. Mater.* 389, 121897. doi:10.1016/j.jhazmat.2019.121897

Cho, D.-W., Jeon, B.-H., Chon, C.-M., Schwartz, F. W., Jeong, Y., and Song, H. (2015). Magnetic Chitosan Composite for Adsorption of Cationic and Anionic Dyes in Aqueous Solution. *J. Ind. Eng. Chem.* 28, 60–66. doi:10.1016/j.jiec.2015.01.023

Coletti, A., Galloni, P., Sartorel, A., Conte, V., and Floris, B. (2012). Salophen and Salen Oxo Vanadium Complexes as Catalysts of Sulfides Oxidation with H2O2: Mechanistic Insights. *Catal. Today* 192, 44–55. doi:10.1016/j.cattod.2012.03.032

Cui, K., Yan, B., Xie, Y., Qian, H., Wang, X., Huang, Q., et al. (2018). Regenerable Urchin-like Fe 3 O 4 @PDA-Ag Hollow Microspheres as Catalyst and Adsorbent for Enhanced Removal of Organic Dyes. *J. Hazard. Mater.* 350, 66–75. doi:10.1016/j.jhazmat.2018.02.011

Dai, H., Chen, Y., Ma, L., Zhang, Y., and Cui, B. (2021). Direct Regeneration of Hydrogels Based on Lemon Peel and its Isolated Microcrystalline Cellulose: Characterization and Application for Methylene Blue Adsorption. *Int. J. Biol. Macromolecules* 191, 129–138. doi:10.1016/j.ijbiomac.2021.09.063

Ding, C., Sun, Y., Wang, Y., Li, J., Lin, Y., Sun, W., et al. (2017). Adsorbent for Resorcinol Removal Based on Cellulose Functionalized with Magnetic Poly(dopamine). *Int. J. Biol. Macromolecules* 99, 578–585. doi:10.1016/j.ijbiomac.2017.03.018

Du, S., Luo, Y., Zuo, F., Li, X., and Liu, D. (2017). Polydopamine-Coated Fe3O4 Nanoparticles as Synergistic Redox Mediators for Catalytic Reduction of Azo Dyes. *Nano* 12, 1750037. doi:10.1142/s1793292017500370

Fu, J., Chen, Z., Wang, M., Liu, S., Zhang, J., Zhang, J., et al. (2015). Adsorption of Methylene Blue by a High-Efficiency Adsorbent (Polydopamine Microspheres): Kinetics, Isotherm, Thermodynamics and Mechanism Analysis. *Chem. Eng. J.* 259, 53–61. doi:10.1016/j.cej.2014.07.101

Ge, F., Ye, H., Li, M.-M., and Zhao, B.-X. (2012). Efficient Removal of Cationic Dyes from Aqueous Solution by Polymer-Modified Magnetic Nanoparticles. *Chem. Eng. J.* 198-199, 11–17. doi:10.1016/j.cej.2012.05.074

Hokkanen, S., Bhatnagar, A., and Sillanpää, M. (2016). A Review on Modification Methods to Cellulose-Based Adsorbents to Improve Adsorption Capacity. *Water Res.* 91, 156–173. doi:10.1016/j.watres.2016.01.008

Hossain, L., Eastman, E., De Rango, M., Raghuwanshi, V. S., Tanner, J., and Garnier, G. (2021). Absorption Kinetics of Nanocellulose Foams: Effect of Ionic Strength and Surface Charge. *J. Colloid Interf. Sci.* 601, 124–132. doi:10.1016/j.jcis.2021.05.092

Islam, M. S., Akter, N., Rahman, M. M., Shi, C., Islam, M. T., Zeng, H., et al. (2018). Mussel-Inspired Immobilization of Silver Nanoparticles toward Antimicrobial Cellulose Paper. *ACS Sustain. Chem. Eng.* 6, 9178–9188. doi:10.1021/acssuschemeng.8b01523

Jo, S., Oh, Y., Park, S., Kan, E., and Lee, S. H. (2017). Cellulose/carrageenan/TiO2 Nanocomposite for Adsorption and Photodegradation of Cationic Dye. *Biotechnol. Bioproc. E* 22, 734–738. doi:10.1007/s12257-017-0267-0

Kim, U.-J., Kim, H. J., Choi, J. W., Kimura, S., and Wada, M. (2017). Cellulose-chitosan Beads Crosslinked by Dialdehyde Cellulose. *Cellulose* 24, 5517–5528. doi:10.1007/s10570-017-1528-y

Lee, C. M., Kubicki, J. D., Fan, B., Zhong, L., Jarvis, M. C., and Kim, S. H. (2015). Hydrogen-Bonding Network and OH Stretch Vibration of Cellulose: Comparison of Computational Modeling with Polarized IR and SFG Spectra. *J. Phys. Chem. B* 119, 15138–15149. doi:10.1021/acs.jpcb.5b08015

Lee, H., Dellatore, S. M., Miller, W. M., and Messersmith, P. B. (2007). Mussel-Inspired Surface Chemistry for Multifunctional Coatings. *Science* 318, 426–430. doi:10.1126/science.1147241

Lee, H., Scherer, N. F., and Messersmith, P. B. (2006). Single-molecule Mechanics of Mussel Adhesion. *Proc. Natl. Acad. Sci.* 103, 12999–13003. doi:10.1073/pnas.0605552103

Lentini, S., Galloni, P., Garcia-Bosch, I., Costas, M., and Conte, V. (2014). Ionic Liquids as Reaction media in Catalytic Oxidations with Manganese and Iron Pyridyl Triazacyclononane Complexes. *Inorg. Chim. Acta* 410, 60–64. doi:10.1016/j.ica.2013.10.016

Li, Y., Xiao, H., Pan, Y., and Wang, L. (2018). Novel Composite Adsorbent Consisting of Dissolved Cellulose Fiber/Microfibrillated Cellulose for Dye Removal from Aqueous Solution. *ACS Sustain. Chem. Eng.* 6, 6994–7002. doi:10.1021/acssuschemeng.8b00829

Lin, J., Chen, S., Xiao, H., Zhang, J., Lan, J., Yan, B., et al. (2020). Ultra-efficient and Stable Heterogeneous Iron-Based Fenton Nanocatalysts for Degrading Organic Dyes at Neutral pH via a Chelating Effect under Nanoconfinement. *Chem. Commun.* 56, 6571–6574. doi:10.1039/d0cc01662d

Lin, J., Wang, H., Ren, E., Song, Q., Lan, J., Chen, S., et al. (2019). Stomatocyte-like Hollow Polydopamine Nanoparticles for Rapid Removal of Water-Soluble Dyes from Water. *Chem. Commun.* 55, 8162–8165. doi:10.1039/c9cc04532e

Lin, X., Ma, W., Wu, H., Cao, S., Huang, L., Chen, L., et al. (2016). Superhydrophobic Magnetic poly(DOPAm-Co-PFOEA)/Fe3O4/cellulose Microspheres for Stable Liquid Marbles. *Chem. Commun.* 52, 1895–1898. doi:10.1039/c5cc08842a

Liu, H., Wei, G., Xu, Z., Liu, P., and Li, Y. (2016). Quantitative Analysis of Fe and Co in Co-substituted Magnetite Using XPS: The Application of Non-linear Least Squares Fitting (NLLSF). *Appl. Surf. Sci.* 389, 438–446. doi:10.1016/j.apsusc.2016.07.146

Liu, L., Gao, Z. Y., Su, X. P., Chen, X., Jiang, L., and Yao, J. M. (2015). Adsorption Removal of Dyes from Single and Binary Solutions Using a Cellulose-Based Bioadsorbent. *ACS Sustain. Chem. Eng.* 3, 432–442. doi:10.1021/sc500848m

Liu, X., Xiao, W., Tao, T., Yang, J., Li, H., Chen, Q., et al. (2021). Transparent, Smooth, and Sustainable Cellulose-Derived Conductive Film Applied for the Flexible Electronic Device. *Carbohydr. Polym.* 260, 117820. doi:10.1016/j.carbpol.2021.117820

Liu, Y., Zeng, G., Tang, L., Cai, Y., Pang, Y., Zhang, Y., et al. (2015). Highly Effective Adsorption of Cationic and Anionic Dyes on Magnetic Fe/Ni Nanoparticles Doped Bimodal Mesoporous Carbon. *J. Colloid Interf. Sci.* 448, 451–459. doi:10.1016/j.jcis.2015.02.037

Llano, T., Arce, C., Ruiz, G., Chenna, N., and Coz, A. (2018). Modelling and Optimization of the Last Two Stages of an Environmentally-Compatible TCF Bleaching Sequence. *BioRes* 13, 6642–6662. doi:10.15376/biores.13.3.6642-6662

Lu, S., Tang, Z., Li, W., Ouyang, X., Cao, S., Chen, L., et al. (2018). Diallyl Dimethyl Ammonium Chloride-Grafted Cellulose Filter Membrane via ATRP for Selective Removal of Anionic Dye. *Cellulose* 25, 7261–7275. doi:10.1007/s10570-018-2052-4

Lu, S., Zhang, X., Tang, Z., Xiao, H., Zhang, M., Liu, K., et al. (2021). Mussel-inspired Blue-Light-Activated Cellulose-Based Adhesive Hydrogel with Fast Gelation, Rapid Haemostasis and Antibacterial Property for Wound Healing. *Chem. Eng. J.* 417, 129329. doi:10.1016/j.cej.2021.129329

Magno, L. M., Hinds, D. T., Duffy, P., Yadav, R. B., Ward, A. D., Botchway, S. W., et al. (2020). Porous Carbon Microparticles as Vehicles for the Intracellular Delivery of Molecules. *Front. Chem.* 8, 576175. doi:10.3389/fchem.2020.576175

Mahmoodi, N. M., Salehi, R., Arami, M., and Bahrami, H. (2011). Dye Removal from Colored Textile Wastewater Using Chitosan in Binary Systems. *Desalination* 267, 64–72. doi:10.1016/j.desal.2010.09.007

Metin, A. Ü., Çiftçi, H., and Alver, E. (2013). Efficient Removal of Acidic Dye Using Low-Cost Biocomposite Beads. *Ind. Eng. Chem. Res.* 52, 10569–10581. doi:10.1021/ie400480s

Mohammed, N., Grishkewich, N., Berry, R. M., and Tam, K. C. (2015). Cellulose Nanocrystal-Alginate Hydrogel Beads as Novel Adsorbents for Organic Dyes in Aqueous Solutions. *Cellulose* 22, 3725–3738. doi:10.1007/s10570-015-0747-3

Mu, C., Zhang, L., Zhang, X., Zhong, L., and Li, Y. (2020). Selective Adsorption of Ag (I) from Aqueous Solutions Using Chitosan/polydopamine@C@magnetic Fly Ash Adsorbent Beads. *J. Hazard. Mater.* 381, 120943. doi:10.1016/j.jhazmat.2019.120943

Otsuka, I., Njinang, C. N., and Borsali, R. (2017). Simple Fabrication of Cellulose Nanofibers via Electrospinning of Dissolving Pulp and Tunicate. *Cellulose* 24, 3281–3288. doi:10.1007/s10570-017-1360-4

Panizza, M., and Cerisola, G. (2009). Direct and Mediated Anodic Oxidation of Organic Pollutants. *Chem. Rev.* 109, 6541–6569. doi:10.1021/cr9001319

Park, H. K., Park, J. H., Lee, H., and Hong, S. (2020). Material-Selective Polydopamine Coating in Dimethyl Sulfoxide. *ACS Appl. Mater. Inter.* 12, 49146–49154. doi:10.1021/acsami.0c11440

Peng, F., Peng, P., Xu, F., and Sun, R.-C. (2012). Fractional Purification and Bioconversion of Hemicelluloses. *Biotechnol. Adv.* 30, 879–903. doi:10.1016/j.biotechadv.2012.01.018

Rastogi, A., Zivcak, M., Sytar, O., Kalaji, H. M., He, X., Mbarki, S., et al. (2017). Impact of Metal and Metal Oxide Nanoparticles on Plant: A Critical Review. *Front. Chem.* 5, 78. doi:10.3389/fchem.2017.00078

Roy, D., Guthrie, J. T., and Perrier, S. (2005). Graft Polymerization: Grafting Poly(styrene) from Cellulose via Reversible Addition−Fragmentation Chain Transfer (RAFT) Polymerization. *Macromolecules* 38, 10363–10372. doi:10.1021/ma0515026

Şerban, I., and Enesca, A. (2020). Metal Oxides-Based Semiconductors for Biosensors Applications. *Front. Chem.* 8, 354. doi:10.3389/fchem.2020.00354

Soares, O. S. G. P., Jardim, E. O., Ramos-Fernandez, E. V., Villora-Picó, J. J., Pastor-Blas, M. M., Silvestre-Albero, J., et al. (2021). Highly N2-Selective Activated Carbon-Supported Pt-In Catalysts for the Reduction of Nitrites in Water. *Front. Chem.* 9, 733881. doi:10.3389/fchem.2021.733881

Srivastava, N., and Roy Choudhury, A. (2021). Green Synthesis of pH-Responsive, Self-Assembled, Novel Polysaccharide Composite Hydrogel and its Application in Selective Capture of Cationic/Anionic Dyes. *Front. Chem.* 9, 761682. doi:10.3389/fchem.2021.761682

Tang, J., Mu, B., Zong, L., Zheng, M., and Wang, A. (2017). Facile and green Fabrication of Magnetically Recyclable Carboxyl-Functionalized Attapulgite/carbon Nanocomposites Derived from Spent Bleaching Earth for Wastewater Treatment. *Chem. Eng. J.* 322, 102–114. doi:10.1016/j.cej.2017.03.116

Tang, Z., Miao, Y., Zhao, J., Xiao, H., Zhang, M., Liu, K., et al. (2021). Mussel-inspired Biocompatible Polydopamine/carboxymethyl Cellulose/polyacrylic Acid Adhesive Hydrogels with UV-Shielding Capacity. *Cellulose* 28, 1527–1540. doi:10.1007/s10570-020-03596-7

Tankhiwale, R., and Bajpai, S. K. (2008). Graft Copolymerization onto Cellulose-Based Filter Paper and its Further Development as Silver Nanoparticles Loaded Antibacterial Food-Packaging Material. *Colloids Surf. B Biointerfaces* 69, 164–168. doi:10.1016/j.colsurfb.2008.11.004

Wang, G., Zhang, J., Lin, S., Xiao, H., Yang, Q., Chen, S., et al. (2020). Environmentally Friendly Nanocomposites Based on Cellulose Nanocrystals and Polydopamine for Rapid Removal of Organic Dyes in Aqueous Solution. *Cellulose* 27, 2085–2097. doi:10.1007/s10570-019-02944-6

Wang, P., Shi, Q., Shi, Y., Clark, K. K., Stucky, G. D., and Keller, A. A. (2009). Magnetic Permanently Confined Micelle Arrays for Treating Hydrophobic Organic Compound Contamination. *J. Am. Chem. Soc.* 131, 182–188. doi:10.1021/ja806556a

Wang, W., Narain, R., and Zeng, H. (2018). Rational Design of Self-Healing Tough Hydrogels: A Mini Review. *Front. Chem.* 6, 497. doi:10.3389/fchem.2018.00497

Xiang, L., Lin, J., Yang, Q., Lin, S., Chen, S., and Yan, B. (2020). Facile Preparation of Hierarchical Porous Polydopamine Microspheres for Rapid Removal of Chromate from the Wastewater. *J. Leather Sci. Eng.* 2, 22. doi:10.1186/s42825-020-00036-x

Xie, Y., Yan, B., Xu, H., Chen, J., Liu, Q., Deng, Y., et al. (2014). Highly Regenerable Mussel-Inspired Fe3O4@Polydopamine-Ag Core-Shell Microspheres as Catalyst and Adsorbent for Methylene Blue Removal. *ACS Appl. Mater. Inter.* 6, 8845–8852. doi:10.1021/am501632f

Xing, R. Z., Li, J. X., Yang, X. G., Chen, Z. W., Huang, R., Chen, Z. X., et al. (2020). Preparation of High-Performance CdS@C Catalyst Using Cd-Enriched Biochar Recycled from Plating Wastewater. *Front. Chem.* 8, 140. doi:10.3389/fchem.2020.00140

Xu, H., Nishida, J., Ma, W., Wu, H., Kobayashi, M., Otsuka, H., et al. (2012). Competition between Oxidation and Coordination in Cross-Linking of Polystyrene Copolymer Containing Catechol Groups. *ACS Macro Lett.* 1, 457–460. doi:10.1021/mz200217d

Xu, Q., Li, X., Lin, Q., Shen, H., Wang, H., and Du, Z. (2020). Improved Efficiency of All-Inorganic Quantum-Dot Light-Emitting Diodes via Interface Engineering. *Front. Chem.* 8, 265. doi:10.3389/fchem.2020.00265

Zeng, H., Hwang, D. S., Israelachvili, J. N., and Waite, J. H. (2010). Strong Reversible Fe3+-Mediated Bridging between Dopa-Containing Protein Films in Water. *Proc. Natl. Acad. Sci.* 107, 12850–12853. doi:10.1073/pnas.1007416107

Zhang, K., Zhang, Y., Yan, D., Zhang, C., and Nie, S. (2018). Enzyme-assisted Mechanical Production of Cellulose Nanofibrils: thermal Stability. *Cellulose* 25, 5049–5061. doi:10.1007/s10570-018-1928-7

Zhang, X., Zhang, C., Lin, Q., Cheng, B., Liu, X., Peng, F., et al. (2019). Preparation of Lignocellulose-Based Activated Carbon Paper as a Manganese Dioxide Carrier for Adsorption and In-Situ Catalytic Degradation of Formaldehyde. *Front. Chem.* 7, 808. doi:10.3389/fchem.2019.00808

Zhang, Y., Wang, J., Shen, G., Duan, J., and Zhang, S. (2020). Template-Free Synthesis of N-Doped Porous Carbon Materials from Furfuryl Amine-Based Protic Salts. *Front. Chem.* 8, 196. doi:10.3389/fchem.2020.00196

Zhang, Y.-X., Guo, X.-Y., Liu, B., Zhang, J.-L., Gao, X.-H., Ma, Q.-X., et al. (2021). Cellulose Modified Iron Catalysts for Enhanced Light Olefins and Linear C5+ α-olefins from CO Hydrogenation. *Fuel* 294, 120504. doi:10.1016/j.fuel.2021.120504

Conflict of Interest: The authors declare that the research was conducted in the absence of any commercial or financial relationships that could be construed as a potential conflict of interest.

Publisher's Note: All claims expressed in this article are solely those of the authors and do not necessarily represent those of their affiliated organizations, or those of the publisher, the editors, and the reviewers. Any product that may be evaluated in this article, or claim that may be made by its manufacturer, is not guaranteed or endorsed by the publisher.